Journal of Materials Chemistry

View Online
Dynamic Article Links

Cite this: *J. Mater. Chem.*, 2011, **21**, 7188

www.rsc.org/materials

PAPER

The crystal structure of the first borohydride borate, $Ca_3(BD_4)_3(BO_3)$†

M. D. Riktor,*[a] Y. Filinchuk,‡[b] P. Vajeeston,[c] E. G. Bardají,[d] M. Fichtner,[d] H. Fjellvåg,[c] M. H. Sørby[a] and B. C. Hauback[a]

Received 6th January 2011, Accepted 17th March 2011
DOI: 10.1039/c1jm00074h

The previously observed intermediate from thermal decomposition of $Ca(BH_4)_2$ has been identified as a calcium borohydride borate with composition $Ca_3(^{11}BD_4)_3(^{11}BO_3)$, synthesized from a double-isotope substituted sample $Ca(^{11}BD_4)_2$. The crystal structure was determined on the basis of Synchrotron Radiation Powder X-ray Diffraction, supported by infrared spectroscopy measurements. The stability of the structure at ambient conditions is confirmed by Density Functional Theory calculations. $Ca_3(^{11}BH_4)_3(^{11}BO_3)$ is the first example of a product from a borohydride oxidation containing both B–H(D) and B–O bonds and represents a novel category of compounds, being completely different from the hydroxoborate products upon borohydride hydrolysis. The result represents hence an important contribution to fundamental boron chemistry.

1. Introduction

The major challenge for the introduction of hydrogen as an energy carrier for mobile applications is a safe and efficient storage of hydrogen. Storage in solid compounds based on lightweight elements is considered the only solution able to meet the long-term goals with respect to the gravimetric hydrogen capacity, given for example by the US DoE and NESSHY-project funded by the European Commission.[1,2] One of the compounds with a high potential for hydrogen storage is the complex hydride $Ca(BH_4)_2$. The hydride has a theoretical capacity of 11.5 wt% H_2 and releases 9.5 wt% according to the following reaction:

$$Ca(BH_4)_2 \rightarrow 2/3CaH_2 + 1/3CaB_6 + 10/3H_2 \qquad (R1)$$

The enthalpy for this reaction is estimated to be 32 kJ mol^{-1} H_2 based on Density Functional Theory (DFT) calculations.[3] This corresponds to an equilibrium pressure of 1 bar below 100 °C, meaning that $Ca(BH_4)_2$ could be considered a low/medium-temperature hydride. Experimental work shows however a more complex behaviour than indicated in (R1) with polymorphic phase transitions and formation of intermediate products.[4–7] So far, four different polymorphs (α-, α′-, γ-, and β-$Ca(BH_4)_2$)[3,8–10] and one intermediate CaB_2H_x-phase[11] have been identified.

One of the intermediate products still being unidentified is the so-called "δ-$Ca(BH_4)_2$". This phase forms by heating the low-temperature modifications α- and γ-$Ca(BH_4)_2$ at relatively high temperatures (above 250 °C).[4,6] Since no gas release could be detected, it has been assumed to represent a novel high-temperature modification of $Ca(BH_4)_2$.[4] However, as the phase always appears as a minority phase in the obtained powder, the identification and structural determination have not yet been possible.

In order to increase the yield of "δ-$Ca(BH_4)_2$", several synthesis routes, such as different heating rates and isotherms at selected temperatures, have been tried. However, none of these attempts were successful. In the current work, a procedure with several repeated heating runs of $Ca(^{11}BD_4)_2$ gave a powder of "δ-$Ca(^{11}BD_4)_2$" in almost pure form. This allowed structure determination by powder X-ray diffraction (PXD) and infrared (IR) spectroscopy. The analysis is somewhat unexpected since it appears that the phase is a result of a partial oxidation. We here report on the crystal structure of the compound $Ca_3(^{11}BD_4)_3(^{11}BO_3)$. The stability of the structure is presently confirmed by DFT calculations.

2. Experimental

$Ca(^{11}BD_4)_2$ was synthesized from a metathesis reaction between $Na^{11}BD_4$ (Katchem Ltd.) and $CaCl_2$ (Sigma-Aldrich). 2.51 g (0.060 mol) of $Na^{11}BD_4$ was ball-milled for 4 h in a Fritsch P6 planetary mill at 600 rpm and added to 3.30 g (0.029 mol) of $CaCl_2$ in 120 ml of THF. The mixture was heated under reflux at 80 °C for 24 h. After cooling to room temperature, the

[a]*Physics Department, Institute for Energy Technology, P. O. Box 40, NO-2027 Kjeller, Norway. E-mail: maritdr@ife.no; Fax: +47 63 81 09 20; Tel: +47 63 80 63 88*
[b]*Swiss-Norwegian Beam Lines at ESRF, BP-220, 38043 Grenoble, France*
[c]*Department of Chemistry, Center for Materials Sciences and Nanotechnology, University of Oslo, P.O. Box 1033 Blindern, N-0315 Oslo, Norway*
[d]*Institute of Nanotechnology, Karlsruhe Institute of Technology (KIT), P. O. Box 3640, D-76021 Karlsruhe, Germany*
† Electronic supplementary information (ESI) available. DOI: 10.1039/c1jm00074h
‡ Present address: Institute of Condensed Matter and Nanosciences, Université Catholique de Louvain, Place L. Pasteur, B-1348, Louvain-la-Neuve, Belgium.

suspension was filtered off and the filtrate was evaporated under vacuum to remove the solvent. The resulting $Ca(^{11}BD_4)_2 \cdot n$THF adduct was then dried at elevated temperature in vacuum (80 °C for 2 h, 100 °C for 2 h, 130 °C for 1 h, and 160 °C for 16 h). The isolated yield with respect to $CaCl_2$ was 1.95 g (84%). The obtained powder mixture contains 64.1 wt% α-, 11.1 wt% β- and 24.8 wt% γ-$Ca(^{11}BD_4)_2$. A doubly isotope labelled starting material (with ^{11}B and D) was used in order to perform neutron diffraction experiments.

The phase of interest was produced by heat treatment of the as-synthesized $Ca(^{11}BD_4)_2$ in a TPD-setup (Thermal Programmed Desorption). 100 mg $Ca(^{11}BD_4)_2$ powder was filled in a stainless steel autoclave under argon and heated to 340 °C at a heating rate of 2 °C min^{-1} under dynamic vacuum. After reaching 340 °C, the sample was immediately cooled down and then kept at 165 °C for 96 h. The heating cycle was repeated 3 times. The synthesis route is elaborated in the Results and discussion section.

Laboratory PXD was performed with a Bruker-AXS D8 Advance diffractometer equipped with a Göbel mirror and a LynxEye™ 1D silicon strip detector. Sample powders were contained in sealed, rotating glass capillaries.

High-resolution Synchrotron Radiation (SR) PXD data were collected at room temperature at the BM01B beam line of the Swiss-Norwegian Beam Lines (SNBL) at the European Synchrotron Radiation Facility (ESRF) in Grenoble, France. The diffractometer was equipped with a Si channel-cut (111) double-crystal monochromator and six scintillation detectors, each with a secondary Si monochromator. The sample was sealed in a 0.5 mm boron–silica glass-capillary, which was rotated during exposure. The measurement was performed using a wavelength of 0.5027 Å.

SR-PXD data with very high counting statistics were collected at the beam line BM01A of SNBL. The sample was filled into a 0.5 mm quartz capillary, and kept in place by a glass rod and mounted in a Swagelok fitting. The capillary was thereafter evacuated with a rotary pump and kept under dynamic vacuum. Two-dimensional diffraction data were collected using an image plate system (MAR345) and an exposure time of 30 s. In order to improve the powder average the capillaries were rotated by 30° during each exposure. 90 s were needed for readout and erasing. The wavelength was 0.7009 Å. The two-dimensional data were calibrated with the NIST LaB_6 standard sample and then integrated into one-dimensional powder diffraction patterns with the program Fit2D.[12] Uncertainties of the integrated intensities were calculated at each 2θ-point by applying Poisson statistics to the intensity data, considering the geometry of the detector, similar to the procedure described by Vogel *et al.*[13]

The programs Dicvol[14] and Chekcell[15] were used for unit cell and space group determination. The global optimization approach with parallel tempering as implemented in the program Fox[16,17] was used for crystal structure determination. Rietveld refinements were carried out using GSAS[18] with the Expgui graphical user-interface.[19] The background was modelled with shifted Chebyschev polynomials with 20 parameters.

IR spectroscopy data were collected with a Perkin-Elmer Spectrum GX FTIR spectrometer. The powder was embedded in KBr pellets (2 mm). The transmission spectra were recorded in the 400–4000 cm^{-1} region, with 2 cm^{-1} resolution.

Density Functional Theory calculations

The quantum-mechanical calculations have been performed in the frame of Density Functional Theory using the generalized gradient approximation (GGA)[20–22] as implemented in the CASTEP code.[23] Norm-conserving pseudopotentials with 600 eV were utilized for all atoms together with a fine mesh of k points, with the energy conversion threshold of 0.01 meV per atom, the maximum displacement of 0.001 Å and the maximum force of 0.03 eV Å^{-1}, yielding a high accuracy for the energy and atomic displacements. For B, O, and Ca atoms the valence region was modelled using the $2s^2$, $2p^1$; $2s^2$, $2p^4$, and $3s^2$, $3p^6$ electrons, respectively. The Perdew–Burke–Ernzerhof 96 and the generalized gradient form (GGA–PBE) of the exchange-correlation functional were applied. Density functional perturbation theory (DFPT) as implemented in CASTEP[24] was used for phonon calculations. For the theoretical simulation the experimental structural parameters were used as starting point, and full geometry optimization has been carried out without any constraints on the atomic positions and unit cell parameters. The phonon calculation was performed using norm-conserving pseudopotentials with an 800 eV energy cut-off for all atoms together with a 12 × 12 × 6 mesh of k points with an 0.01 1/Å q-vector grid spacing for the interpolation.

3. Results and discussion

Synthesis of the unknown phase

An earlier *in situ* SR-PXD study showed that a mixture of α-, β- and γ-$Ca(BH_4)_2$ had fully transformed into β-$Ca(BH_4)_2$ and the uncharacterized "δ"-phase at 340 °C. Moreover, it was clear that the "δ"-phase formed much more readily from the low-temperature phases α and γ than from the β-phase (ref. 4 and 6). Several studies have earlier shown that the β-modification slowly transforms to the low-temperature α-modification upon cooling. The amount formed depends on several parameters such as cooling rate, maximum heating temperature and duration of the annealing.[9,25]

In order to produce a sample with large amount of the "δ"-phase for structural characterization, a temperature cycling approach was attempted. As-synthesized $Ca(^{11}BD_4)_2$ was heated at 2 °C min^{-1} to 340 °C to produce a mixture of β-$Ca(^{11}BD_4)_2$ and the δ-phase. The sample was then kept at 165 °C for 96 hours in order to regain some of the low-temperature modifications. After cooling to ambient temperature, some material was then removed for PXD measurement (Fig. 1b). The formation of a notable amount of the "δ"-phase was confirmed. The remaining $Ca(^{11}BD_4)_2$ was partly in the β-modification, but a significant amount had been transformed to the low-temperature modifications, mainly the α-phase. Two further heating cycles of heating to 340 °C at 2 °C min^{-1} then at 165 °C for 96 hours were performed. The product after 3 cycles contained the "δ"-phase, identified below as $Ca_3(^{11}BD_4)_3(^{11}BO_3)$, in almost pure form.

The source of oxygen for the formation of $Ca_3(^{11}BD_4)_3(^{11}BO_3)$ remains unknown. However, it is clear that it must either originate from impurities in the as-synthesised material or from the atmosphere through a leak in the setup. The fact that the "δ"-phase is observed by many groups with extensive experience in handling air-sensitive materials and in different kind of

supposedly oxygen-free environments indicates that $Ca(BH_4)_2$ is prone to incorporate oxygen-containing impurities during synthesis. Indeed, the authors have recently reported quasi-elastic neutron spectroscopy investigations of $Ca(BH_4)_2$ which indicate that the material contained remains of organic adducts (THF) even after thorough drying under vacuum at elevated temperatures.[26]

Subsequent attempts to reproduce the phase were done on a different batch of $Ca(^{11}BD_4)_2$, as the original batch was exhausted in the first experiment. These experiments gave just small yields during the first heating, and the amount did not increase upon repeated heating cycles. These results give no direct indication of the oxygen source for the massive formation of $Ca_3(^{11}BD_4)_3(^{11}BO_3)$ in the first experiments since the difference in "δ"-phase formation could be either due to a more impure first batch or due to a leak in the setup in the first experiment which was not present in the later experiments. However, since some $Ca_3(BH_4)_3(BO_3)$ is always formed, and the TPD setup shows no sign of leakage for other investigated systems, it is believed that at least some of the oxygen comes from impurities in the first experiment and that the smaller amounts of $Ca_3(^{11}BD_4)_3(^{11}BO_3)$ formed in the subsequent experiments with the new batch of materials are entirely due to oxygen containing impurities. This must be further investigated by careful examination of the starting material by spectroscopic techniques and also by thermal decomposition of $Ca(BH_4)_2$ under controlled exposure to the atmosphere.

As the attempts to synthesize samples in larger quantities were not successful, neutron diffraction data could not be collected.

We have previously suggested that the "δ"-phase could represent a high temperature modification of $Ca(BH_4)_2$ since no gas release was observed during its formation.[4] For the corresponding deuteride, the yield of the "δ"-phase is significantly higher than for the hydride, and the TPD-curve shows gas release in the temperature region where "δ-$Ca(^{11}BD_4)_2$" is formed (Fig. 2). This observation supports that the "δ"-phase is not a $Ca(BH_4)_2$ modification.

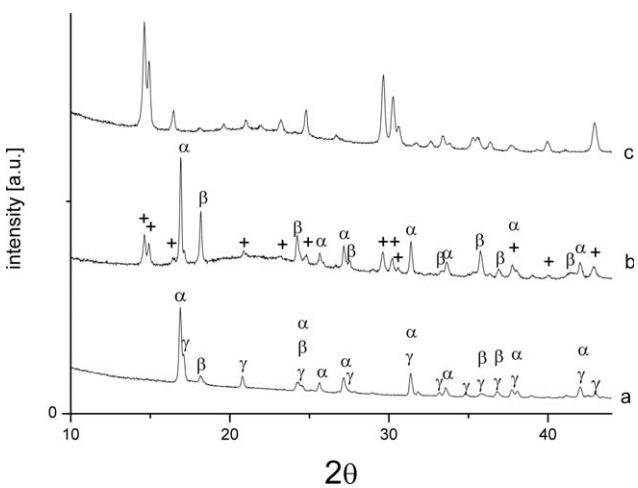

Fig. 1 PXD-data for (a) the as-synthesized $Ca(^{11}BD_4)_2$, (b) after one heating cycle and (c) after three heating cycles. The labels α, β and γ refer to $Ca(^{11}BD_4)_2$ modifications. Bragg peaks from $Ca_3(^{11}BD_4)_3(^{11}BO_3)$ are marked +. In pattern (c) a small peak from β-$Ca(^{11}BD_4)_2$ is detected at 18°. All other peaks stem from $Ca_3(^{11}BD_4)_3(^{11}BO_3)$.

Characterisation of the $Ca_3(^{11}BD_4)_3(^{11}BO_3)$ phase

The structure was indexed from 17 resolved Bragg peaks in the range $2\theta = 4.80$–$14.91°$ ($d = 5.998$–1.996 Å) based on high resolution SR-PXD data. The best figure of merit was obtained for an orthorhombic cell with unit cell parameters $a = 8.995$ Å, $b = 8.052$ Å and $c = 11.767$ Å. The same cell was also obtained by indexing the image plate data. Systematic absences suggest one of the space groups *Cmcm*, *C*2*cm* or *Cmc*2_1. The structure was solved in *Cmc*2_1 by using FOX[16,17] on the image plate data. During the structure solution two positions of calcium and six positions of boron were optimized. Variable occupancy was used for the light atoms, finding higher scattering power in some positions that later were identified as oxygen atoms. Antibump restraints on the shortest D–D and Ca–D distances helped to find the orientation of the BD_4 group.

The structure was refined according to the Rietveld method using the software GSAS. Two datasets were refined, one from the high resolution SR (BM01B) and one from the image plate setup (BM01A). The refinements were performed with soft constraints on B–D and D–D distances within the BD_4 complex owing to weak scattering from the deuterium atoms. The refinement converged at $R_{wp} = 2.96\%$ (background not subtracted). The obtained fit and reflection profiles are shown in Fig. 3. Quantitative analysis gave 1.7 wt% β-$Ca(^{11}BD_4)_2$ and 98.3 wt% $Ca_3(^{11}BD_4)_3(^{11}BO_3)$. Examination of the resulting structure and analysis by Platon[27] did not find any higher crystallographic symmetry. The refined structural parameters and selected interatomic distances are given in Tables 1 and 2, respectively. The structure is shown in Fig. 4. The calculated unit cell dimensions and positional parameters at 0 K and ambient pressure from DFT were in good agreement with the experimental values obtained at room temperature (Table 1). The deviations between theoretical and experimental unit cell parameters *a* and *b* are less than 0.9% and the overestimation of 1.6% in the *c* direction is within typical error bars for DFT modeling. In order to understand the stability of the

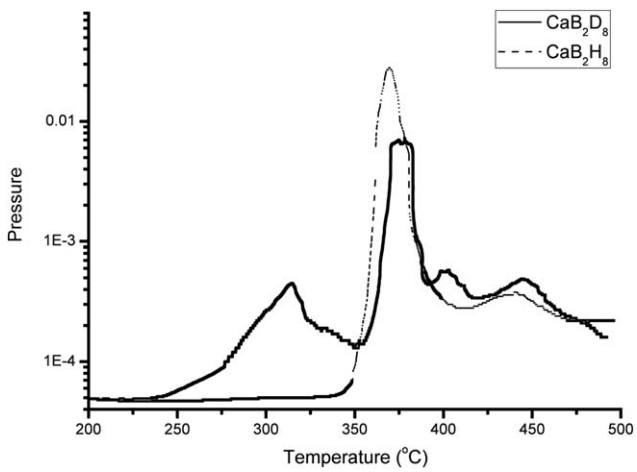

Fig. 2 Thermal desorption curves for $Ca(BH_4)_2$ and $Ca(^{11}BD_4)_2$. The "δ"-phase is formed in the temperature region 250–340 °C.

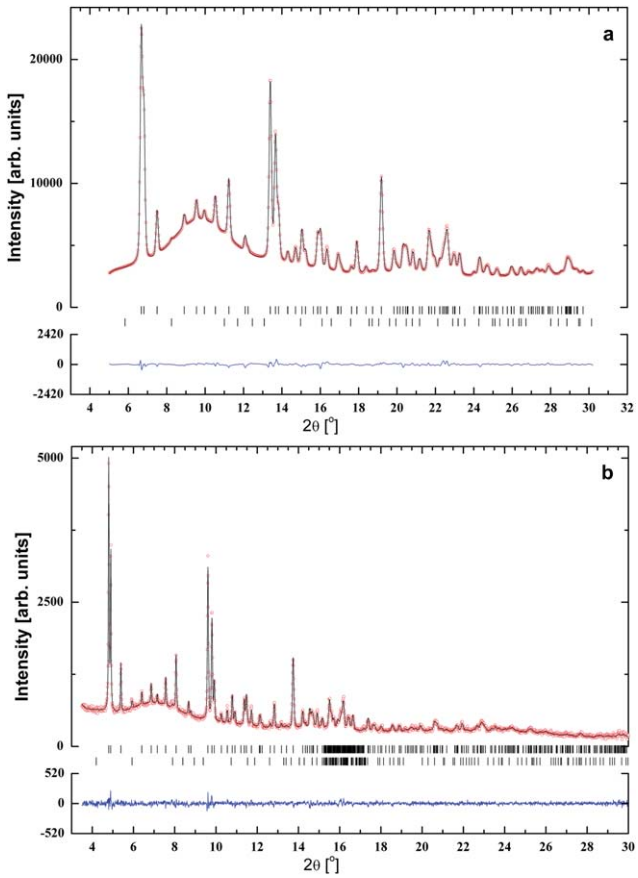

Fig. 3 Rietveld refinement profiles for $Ca_3(^{11}BD_4)_3(^{11}BO_3)$ measured with (a) an image-plate set-up at BM01A and (b) a high resolution diffractometer at BM01B. The figures show observed (circles), calculated (upper line) and difference (bottom line) profiles. Bars indicate the position of Bragg reflections for $Ca_3(^{11}BD_4)_3(^{11}BO_3)$ (upper) and β-Ca $(^{11}BD_4)_2$.

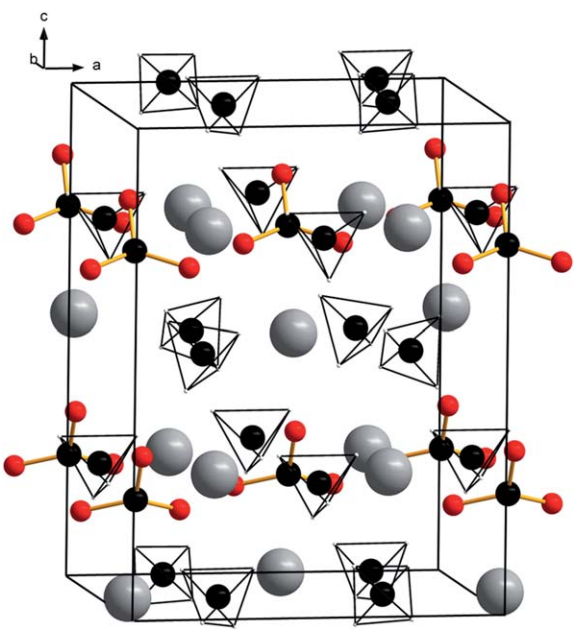

Fig. 4 The crystal structure of $Ca_3(^{11}BD_4)_3(^{11}BO_3)$. Ca-atoms are shown as large spheres, oxygen as red spheres, and BD_4 anions as polyhedra.

experimentally identified phase, the phonon density of states for $Ca_3(BD_4)_3(BO_3)$ was calculated at the theoretical equilibrium volume (see Fig. S1 in the ESI†). For this phase no imaginary frequency was identified. This indicates that the experimentally identified structure is the ground-state structure for the $Ca_3(BD_4)_3(BO_3)$ composition, or at least it is a dynamically stable compound.

Fig. 5 presents IR spectra of the starting material ($Ca(^{11}BD_4)_2$) and of the cycled powder containing mostly $Ca_3(^{11}BD_4)_3(^{11}BO_3)$. The bands around ~1100 cm^{-1} and ~2300 to 2400 cm^{-1} can be assigned to B–H modes, while the bands around ~800 cm^{-1} and 1700 cm^{-1} are related to B–D bending and stretching modes, respectively. It is hence evident that the sample contained both ^1H (H) and ^2H (D). This is actually expected since the starting materials for synthesis of $Ca(^{11}BD_4)_2$ are not available in an isotope-pure form.

The cycled powder shows clear bands from the B–H and B–D modes of the BH_4/BD_4-complexes, thus confirming the presence of $BD_{4-x}H_x$ entities in the sample. In addition to the modes from B–H and B–D vibrations, three new bands appear; a weak band at 615 cm^{-1}, a relatively strong doublet at 768/776 cm^{-1} and a strong band at 1264 cm^{-1}. These bands can be assigned to the asymmetric bending (ν_4/ν_6), the symmetric bending (ν_3), and the asymmetric stretching (ν_2/ν_5), respectively, of the internal vibrations of the BO_3^{3-} anion. The labelling ν_1–ν_6 is based on the vibrational modes of a free BO_3^{3-} anion belonging to the symmetry group C_s. The splitting of the band from the symmetric bending (ν_3) is due to crystal field effects. The observed frequencies correspond very well to the frequencies obtained from the current DFT calculations (Table 3). The total Density of States (DOS) at the equilibrium volumes for the $Ca_3(^{11}BD_4)(^{11}BO_3)$ structure is given in the ESI† (Fig. S2). Similar to $Ca(BH_4)_2$, $Ca_3(^{11}BD_4)(^{11}BO_3)$ also has a finite energy gap (6 eV, *i.e.* direct band gap) between the valence band and the conduction band. Hence, they are both insulators.

Structure description

$Ca_3(^{11}BD_4)_3(^{11}BO_3)$ can be described as a calcium borohydride borate with Ca^{2+} cations surrounded by both BD_4^- and BO_3^{3-} anions. The Ca cation is coordinated by four BD_4^- anions and two BO_3^{3-} anions in a strongly distorted octahedral configuration. There are two non-equivalent Ca-atoms in the unit cell. The Ca(1) atom in the 4*a* Wychoff site is coordinated by one type BD_4 anion with Ca(1)–BD_4 distances of 3.009 and 3.118 Å. The Ca(1)–BO_3 distances are 2.71 and 3.34 Å with a $B(O_3)$–Ca(1)–$B(O_3)$ angle of 155°. The Ca(2) cation in the 8*b* site is coordinated by two different BD_4 anions with four different Ca(2)–BD_4 distances ranging from 2.949 Å to 3.051 Å. The Ca(2)–BO_3 distances are 2.62 Å and 3.44 Å, and the $B(O_3)$–Ca(2)–$B(O_3)$ angle is 170°.

The Ca atoms in the different $Ca(BH_4)_2$ modifications are octahedrally coordinated by six complex anions. The $Ca(BH_4)_2$ modifications differ with respect to the orientation of these BH_4 groups and to octahedral deformations.[8,9] The tetragonal β-modification is least distorted with four BH_4 anions in the plane around Ca and with B–B distances between 3.91 and 4.37 Å. The orthorhombic low temperature α and γ modifications are more distorted with larger variations in the B–B

Table 1 Refined and calculated structural parameters for $Ca_3(^{11}BD_4)_3(^{11}BO_3)$. Space group $Cmc2_1$ (no. 36); $Z = 4$. Estimated standard deviations in parentheses

		Experimental parameters $a = 8.9981$ (2) Å, $b = 8.0562$ (2) Å, $c = 11.7678$ (3) Å			Calculated parameters $a = 9.07$ Å, $b = 8.13$ Å, $c = 11.95$ Å		
Atom	Site	x	y	z	x	y	z
Ca(1)	4*a*	0	0.0778 (3)	0.0390 (8)	0	0.0755	0.0388
Ca(2)	8*b*	0.2331 (2)	0.7782 (2)	0.2684 (2)	0.2309	0.7779	0.2693
B(1)	4*a*	0	1.027 (2)	0.7577 (4)	0	1.0005	0.7640
O(1)	4*a*	0	1.1196 (9)	0.8435 (3)	0	1.1158	0.8443
O(2)	8*b*	−0.1313 (4)	0.9491 (8)	0.7186 (3)	−0.1280	0.9512	0.7179
B(2)	4*a*	0	0.488 (1)	0.7743 (4)	0	0.5053	0.7800
D(1)	8*b*	0.1042 (4)	0.469 (1)	0.8277 (4)	0.1064	0.4906	0.8408
D(2)	4*a*	0	0.6219 (9)	0.7395 (4)	0	0.6409	0.7361
D(3)	4*a*	0	0.396 (1)	0.7001 (4)	0	0.4044	0.7050
B(3)	8*b*	0.7208 (6)	0.7189 (8)	0.5180 (4)	0.7252	0.7189	0.5160
D(4)	8*b*	0.6327 (8)	0.767 (1)	0.5822 (4)	0.6239	0.73346	0.5816
D(5)	8*b*	0.665 (1)	0.635 (1)	0.4539 (4)	0.6906	0.6195	0.4446
D(6)	8*b*	0.772 (1)	0.8317 (9)	0.4738 (4)	0.7408	0.8539	0.4745
D(7)	8*b*	0.8100 (8)	0.649 (1)	0.5672 (4)	0.8373	0.6688	0.5608

distances. In the proposed structure for $Ca_3(^{11}BD_4)_3(^{11}BO_3)$ the B–B distances between the four BD_4-complexes are in the range 3.97–5.02 Å for one octahedron and 4.16–4.34 Å for the second. The Ca–Ca separations of 3.958 and 4.185 Å are intermediate of those reported for $Ca(BH_4)_2$ modifications (4.33–4.41 Å)[8] and $Ca_3(BO_3)_2$ (3.4 Å).[28]

The BO_3^{3-} anion has a distorted triangular geometry with slightly different B–O distances (1.26 and 1.41 Å) and O–B–O angles 113° and 121°. The O–O distances within the unit are 2.33 and 2.36 Å. Within experimental uncertainties, this corresponds well to the expected trigonal-planar unit, however, with the B atom slightly displaced towards O1 resulting in one shortened B–O bond. Each BO_3^{3-} anion is coordinated by six Ca-atoms. The Ca–O distances are in the range 2.277–2.452 Å, and each oxygen atom is coordinated to three Ca and one B atom. For comparison, the BO_3^{3-} anion in $Ca_3(BO_3)_2$ is undistorted triangular with just a slight deviation from planarity. The B–O distance is 1.380 Å, and the O atoms are penta-coordinated by four Ca-atoms (2.347, 2.431, 2.440 and 2.732 Å) and one B-atom (1.384 Å).[28]

The structure contains two crystallographically independent BD_4 complexes. Each BD_4 anion is coordinated by four Ca atoms. In $Ca(BH_4)_2$ the coordination number for the BH_4 anions is 3, and the reported Ca–B distances are in the range 2.816–2.976 Å.[8–10] The slightly increased Ca–BD_4 distances observed in the title compound (2.949–3.118 Å) fit well with the increased coordination number. The B–H/D distances are within the limits reported for the various $Ca(BH_4)_2$ polymorphs.

Table 2 Selected interatomic distances in $Ca_3(^{11}BD_4)_3(^{11}BO_3)$. Estimated standard deviations in parentheses

Ca–Ca	3.958 (7)–4.185 (7) Å
Ca–B (BD_4)	2.949 (5)–3.118 (6) Å
Ca–B (BO_3)	2.623 (9) Å, 2.71 (1) Å
Ca–O	2.277 (6)–2.452 (6) Å
B–O	1.26 (1) Å, 1.415 (8) Å
B–D	1.130 (8)–1.162 (8) Å
D–D (within BD_4)	1.863 (6)–1.876 (9) Å

A search in the ICSD database[29] did not reveal any compounds containing both B–H and B–O bonds. To our knowledge this is the first identified intermediate resulting from a partial oxidation of a metal borohydride. This is completely different from the hydroxoborate products of borohydride hydrolysis, *e.g.* $Na(B(OH)_4)$.[30] The observed coexistence of BD_4 and BO_3 anions is highly interesting, and may lead to future insight to the reaction mechanisms of borohydride oxidation. Understanding and control of borohydride hydrolysis and oxidation reactions represent main challenges both in the generation of hydrogen by hydrolysis (chemical hydrogen storage)[30,31] and in direct borohydride fuel cells, where competition between hydrolysis and electro-oxidation of BH_4^- is a main obstacle.[32] A complete understanding of the oxidation mechanisms, including formation of intermediate phases such as $Ca(BH_4)_3(BO_3)$, could greatly aid the efforts to control and improve the performances of these systems.

At present the physical and chemical properties of the novel calcium borohydride borate are unknown. However, being a mixed anion compound, it is likely that the compound exhibits properties resembling both borohydrides and borates. Further

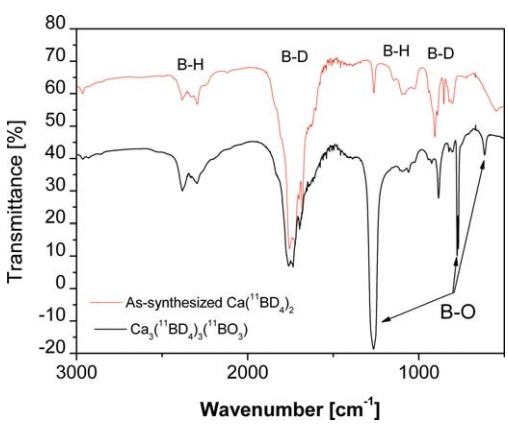

Fig. 5 IR-spectra of the as-synthesized $Ca(^{11}BD_4)_2$ (red line) and of the cycled material containing mostly $Ca_3(^{11}BD_4)_3(^{11}BO_3)$ (black line).

Table 3 Observed and calculated frequencies for internal vibrations of the BO_3-anion. The calculated bands from the symmetric stretching vibrations at 905 and 906 cm^{-1} are not observed due to too small changes in dipole momentum. The modes of the asymmetric vibrations (ν_2/ν_5) and (ν_4/ν_6) cannot be separated in the experimental spectrum due to limited resolution. The site groups in brackets refer to the C_{2v} site group for the complete unit cell

Type of B–O vibration	C_s site group	Exp. frequencies/cm^{-1}	Calculated frequencies/cm^{-1}
ν_1	A′		904.73 (A1)
			906.15 (B1)
ν_2	A′	1264	1295.35 (A1)
ν_5	A″		1303.12 (B2)
ν_3	A′	768	777.30 (A1)
		776	780.64 (B1)
ν_4	A′	615	590.96 (A1)
ν_6	A″		591.08 (B2)

investigations of this novel category of compounds by optimizing synthesis methods, followed by studies of reaction mechanisms and material properties would certainly be of great interest.

4. Conclusion

The material earlier described as "δ-$Ca(BH_4)_2$" has been synthesized for the first time in almost pure form. The compound has been identified as $Ca_3(^{11}BD_4)_3(^{11}BO_3)$. The crystal structure is determined from SR-PXD data and refined according to the Rietveld method. IR spectra and DFT calculations support the proposed structure model. The compound represents a novel category, *i.e.* a calcium borohydride borate. To our knowledge this is the first identified intermediate of metal borohydride oxidation, being completely different to the hydroxoborate products from borohydride hydrolysis. This discovery is considered to be of great interest from a fundamental boron chemistry point of view, and could possibly provide clues to understanding of the reaction mechanisms of borohydride oxidation.

Acknowledgements

Partial funding by the European Commission DG Research (contract SES6-2006-51827/NESSHY) and the Helmholtz initiative "FuncHy" is gratefully acknowledged by the authors. The skilful assistance from the project team at the Swiss Norwegian Beam Line at ESRF is gratefully acknowledged.

References

1 *US Department of Energy Hydrogen Program*, http://www.hydrogen.energy.gov/.
2 *European Commission DG Research*, http://www.nesshy.net.
3 K. Miwa, M. Aoki, T. Noritake, N. Ohba, Y. Nakamori, S. Towata, A. Zuttel and S. Orimo, *Phys. Rev. B: Condens. Matter Mater. Phys.*, 2006, **74**, 155122.
4 M. D. Riktor, M. H. Sorby, K. Chlopek, M. Fichtner, F. Buchter, A. Zuettel and B. C. Hauback, *J. Mater. Chem.*, 2007, **17**, 4939–4942.
5 M. Aoki, K. Miwa, T. Noritake, N. Ohba, M. Matsumoto, H. W. Li, Y. Nakamori, S. Towata and S. Orimo, *Appl. Phys. A: Mater. Sci. Process.*, 2008, **92**, 601–605.
6 A. Nickels and W. I. F. David, in *Symposium on Metal-Hydrogen Systems, Reykjavik, Iceland*, 2008.
7 Y. Kim, D. Reed, Y. S. Lee, J. Y. Lee, J. H. Shim, D. Book and Y. W. Cho, *J. Phys. Chem. C*, 2009, **113**, 5865–5871.
8 Y. Filinchuk, E. Ronnebro and D. Chandra, *Acta Mater.*, 2009, **57**, 732–738.
9 F. Buchter, Z. Lodziana, A. Remhof, O. Friedrichs, A. Borgschulte, P. Mauron, A. Zuttel, D. Sheptyakov, L. Palatinus, K. Chlopek, M. Fichtner, G. Barkhordarian, R. Bormann and B. C. Hauback, *J. Phys. Chem. C*, 2009, **113**, 17223–17230.
10 F. Buchter, Z. Lodziana, A. Rernhof, O. Friedrichs, A. Borgschulte, P. Mauron, A. Zuttel, D. Sheptyakov, G. Barkhordarian, R. Bormann, K. Chlopek, M. Fichtner, M. Sorby, M. Riktor, B. Hauback and S. Orimo, *J. Phys. Chem. B*, 2008, **112**, 8042–8048.
11 M. D. Riktor, M. H. Sorby, K. Chlopek, M. Fichtner and B. C. Hauback, *J. Mater. Chem.*, 2009, **19**, 2754–2759.
12 A. P. Hammersley, S. O. Svensson, M. Hanfland, A. N. Fitch and D. Hausermann, *High Pressure Res.*, 1996, **14**, 235–248.
13 L. Ehm, S. Vogel, K. Knorr and G. Braun, *Adv. X-Ray Anal.*, 2002, **45**, 31–33.
14 A. Boultif and D. Louer, *J. Appl. Crystallogr.*, 1991, **24**, 987–993.
15 B. Bochu and J. Laugier, *LMPG-Suite, Suite of Programs for the Interpretation of X-ray Experiments*, http://www.ccp14.ac.uk/tutorial/lmgp.
16 V. Favre-Nicolin and R. Cerny, *J. Appl. Crystallogr.*, 2002, **35**, 734–743.
17 V. Favre-Nicolin and R. Cerny, *Z. Kristallogr.*, 2004, **219**, 847–856.
18 A. C. Larson and R. B. Von Dreele, *GSAS. Report No. LAUR 86-748*, Los Alamos National Laboratory, New Mexico, USA, 1994.
19 B. H. Toby, *J. Appl. Crystallogr.*, 2001, **34**, 210–213.
20 J. P. Perdew, in *Electronic Structure of Solids*, ed. P. Ziesche and H. Eschrig, Akademie, Berlin, 1991, p. 11.
21 J. P. Perdew, K. Burke and Y. Wang, *Phys. Rev. B: Condens. Matter Mater. Phys.*, 1996, **54**, 16533–16539.
22 J. P. Perdew, K. Burke and M. Ernzerhof, *Phys. Rev. Lett.*, 1996, **77**, 3865–3868.
23 S. J. Clark, M. D. Segall, C. J. Pickard, P. J. Hasnip, M. J. Probert, K. Refson and M. C. Payne, *Z. Kristallogr.*, 2005, **220**, 567–570.
24 K. Refson, P. R. Tulip and S. J. Clark, *Phys. Rev. B: Condens. Matter Mater. Phys.*, 2006, **73**, 155114.
25 M. Fichtner, K. Chlopek, M. Longhini and H. Hagemann, *J. Phys. Chem. C*, 2008, **112**, 11575–11579.
26 D. Blanchard, M. D. Riktor, J. B. Maronsson, H. S. Jacobsen, J. Kehres, D. Sveinbjornsson, E. G. Bardaji, A. Leon, F. Juranyi, J. Wuttke, B. C. Hauback, M. Fichtner and T. Vegge, *J. Phys. Chem. C*, 2010, **114**, 20249–20257.
27 A. L. Spek, *J. Appl. Crystallogr.*, 2003, **36**, 7–13.
28 A. Vegas, *Acta Crystallogr., Sect. C: Cryst. Struct. Commun.*, 1985, **41**, 1689–1690.
29 *Inorganic Crystal Structure Database*, http://www.fiz-karlsruhe.de/icsd.html.
30 J. H. Wee, K. Y. Lee and S. H. Kim, *Fuel Process. Technol.*, 2006, **87**, 811–819.
31 U. B. Demirci, O. Akdim and P. Miele, *J. Power Sources*, 2009, **192**, 310–315.
32 J. Hong, B. Fang, C. S. Wang and K. Currie, *J. Power Sources*, 2006, **161**, 753–760.